Crystalline ZrO_2 Monoliths with Well-Defined Macropores and Mesostructured Skeletons Prepared by Combining the Alkoxy-Derived Sol–Gel Process Accompanied by Phase Separation and the Solvothermal Process

Junko Konishi,[†] Koji Fujita,*[,†,‡] Satoshi Oiwa,[†] Kazuki Nakanishi,[§] and Kazuyuki Hirao[†]

Department of Material Chemistry, Graduate School of Engineering, Kyoto University, Nishikyo-ku, Kyoto 615-8510, Japan, PRESTO, Japan Science and Technology Agency (JST), 4-1-8 Honcho Kawaguchi, Saitama 332-0012, Japan, Department of Chemistry, Graduate School of Science, Kyoto University, Kitashirakawa, Sakyo-ku, Kyoto 606-8502, Japan

Received November 26, 2007. Revised Manuscript Received January 18, 2008

We have successfully prepared multiscale porous crystalline zirconia (ZrO_2) monoliths by combining the alkoxy-derived sol–gel process accompanied by phase-separation and the solvothermal process. The gelation can be controlled by the addition of *N*-methylformamide to the starting solution, while the phase separation is induced by the incorporation of poly(ethylene oxide). Amorphous ZrO_2 monolithic gels with well-defined bicontinuous macropores and microstructured skeletons are obtained when the transient structure of polymerization-induced phase separation is fixed by the gelation. The size of the macropores is controlled in the range of 300 nm to 2 μm by adjusting the amount of poly(ethylene oxide). The solvent exchange of the mother liquor in the as-gelled wet specimens with absolute ethanol, followed by the solvothermal treatment at temperatures above 210 °C, brings about the formation of mesopores and stabilizes tetragonal ZrO_2 nanocrystals without disturbing the macroporous morphology. The resultant macro-mesoporous crystalline ZrO_2 gels possess the surface area over 200 $m^2\ g^{-1}$.

Introduction

Hierarchically structural porous metal oxides on multiple scales have attracted considerable attention for both fundamental and practical reasons.[1] Especially in applications that utilize liquid-phase reactions such as catalyst–supports and separations, macroporous materials with mesotexture are highly desirable, because the macroporous channels allow facile fluid transport, while mesopores enlarge the surface area that assists the contacts of the fluid and the solid surface. Typically, macro-mesoporous metal oxides have been prepared via dual templating approaches,[2–6] in which self-assembling surfactants or amphiphilic block copolymers are used as mesotemplates, and latex spheres, emulsion droplets, or polymer membranes as macrotemplates. Recent studies have also revealed that the formation of macro-mesoporous structures in metal oxides is possible in the presence of a single surfactant[7] and even in a template-free condition.[8] Among a variety of metal oxides, zirconia (ZrO_2) gathers the increasing interest in applications as catalyst–supports, chemical sensors, and separation media.[9–12] Template strategies allow the fabrication of macro-mesoporous ZrO_2;[6,7] however, the resultant materials are dried to powders or highly cracked and fragile monoliths, which would limit their utility in areas where processing or application dictates some structural form with moderate mechanical strength. Thus, it still remains a challenge to integrate the multiscale porous structures into a ZrO_2 monolith.

On the other hand, a sol–gel method accompanied by phase separation is well established as a technique to produce silica (SiO_2)-based monolithic gels with multiscale porous structures.[13,14] In this approach, the phase separation and sol–gel transition concur by the polymerization reaction to produce a wet gel with a bicontinuous structure, in which each of gel-rich and solvent-rich phases is interconnected on the length scale of micrometer. Subsequent solvent exchange with a basic aqueous solution and heat treatment yield mesopores via Ostwald ripening, without essentially disturbing the macroporous structures. The resultant macro-mesoporous SiO_2 monoliths exhibit some remarkable properties as the stationary phase of high-performance liquid

* Corresponding author. E-mail: fujita@dipole7.kuic.kyoto-u.ac.jp. Tel.: +81-75-383-2432. Fax: +81-75-383-2420.
[†] Department of Material Chemistry, Kyoto University.
[‡] PRESTO, JST.
[§] Department of Chemistry, Kyoto University.

(1) Yuan, Z.; Su, B. *J. Mater. Chem.* **2006**, *16*, 663.
(2) Holland, B.; Blanford, C.; Stein, A. *Science* **1998**, *281*, 538.
(3) Deng, W.; Toepke, M.; Shanks, B. *Adv. Funct. Mater.* **2003**, *13*, 61.
(4) Yuan, Z.; Ren, T.; Su, B. *Adv. Mater.* **2003**, *15*, 1462.
(5) Grosso, D.; Illia, G.; Crepaldi, E.; Charleux, B.; Sanchez, C. *Adv. Funct. Mater.* **2003**, *13*, 37.
(6) Chen, H.; Gu, J.; Shi, J.; Liu, Z.; Gao, J.; Ruan, M.; Yan, D. *Adv. Mater.* **2005**, *17*, 2010.
(7) Blin, J.; Leonard, A.; Yuan, Z.; Gigot, L.; Vantomme, A.; Cheetham, A.; Su, B. *Angew. Chem., Int. Ed.* **2003**, *42*, 2872.
(8) Collins, A.; Carriazo, D.; Davis, S.; Mann, S. *Chem. Commum.* **2004**, 568.
(9) Tanabe, K. *Mater. Chem. Phys.* **1985**, *13*, 347.
(10) Mercera, P.; Vanommen, J.; Doesburg, E.; Burggaaf, A.; Ross, J. *Appl. Catal.* **1991**, *71*, 363.
(11) Wirth, H.; Hearn, M. *J. Chromatogr., A* **1995**, *711*, 223.
(12) Trudinger, U.; Muller, G.; Unger, K. *J. Chromatogr.* **1990**, *535*, 111.
(13) Nakanishi, K. *J. Porous Mater.* **1997**, *4*, 67.
(14) Nakanishi, K.; Soga, N. *J. Am. Ceram. Soc.* **1991**, *74*, 2518.

10.1021/cm703351d CCC: $40.75
Published on Web 03/01/2008

chromatography, compared to the conventional particle-packed systems.[15–19] Since the preparation of monolithic materials via the sol–gel route requires a relatively high concentration of precursors, the reactivity of precursors significantly affects the feasibility of producing uniform, crack-free monoliths. The successful preparation of porous SiO_2 monoliths under template-free conditions is primarily due to the ease of controlling the hydrolysis and polycondensation of silicon alkoxides. In contrast, transition metal alkoxides such as titanium and zirconium alkoxides are highly reactive, and thus, the structural development during the hydrolysis and polycondensation is usually hard to be controlled because of the rapid polymerization.[20] A common strategy to tackle this problem is to reduce the reactivity of precursors either by the use of a strong acid such as hydrochloric acid and nitric acid or by the addition of a chelating agent such as acetic acid,[21–23] but the challenge remains as to how to induce the homogeneous gelation throughout the solution.

We recently developed an alkoxy-derived sol–gel route to synthesize robust, multiscale porous titania (TiO_2) monoliths.[24] In this approach, a strong acid such as hydrochloric acid is used as an inhibitor for polymerization reaction, and formamide as an acid scavenger to raise the solution pH gradually. The slow and uniform increase in the solution pH drives the hydrolysis and condensation of alkoxy-derived oligomers and ultimately results in the homogeneous gelation to produce a monolithic gel. When the phase separation is induced parallel to the gelation, monolithic gels with bicontinuous macropores and mesostructured anatase TiO_2 skeletons can be obtained in large dimensions such as a circular cylinder with a diameter of 4 mm and a length of 50 mm. Very recently, a similar sol–gel approach was reported by Backlund et al.[25] to fabricate macro-mesoporous TiO_2 monoliths. Thus, this technique would be very useful for designing multiscale porous ZrO_2 monoliths.

In this study, a trial of preparing macro-mesoporous ZrO_2 monoliths via the alkoxy-derived sol–gel process accompanied by phase separation is demonstrated. The preliminary experiments revealed that two major obstacles existed for the fabrication of macro-mesoporous ZrO_2 monoliths via the phase separation route. One obstacle is higher reactivity of zirconium alkoxides compared to titanium alkoxides. This is due to larger positive partial charge on the zirconium atom, which enhances the nucleophilic attack of the attacking molecule to zirconium atom. For the purpose of suppressing the high reactivity of zirconium alkoxides, we here utilize *N*-methylformamide as the acid scavenger, instead of formamide used in the TiO_2 systems.[24] In the acid condition, *N*-methylformamide is more slowly hydrolyzed than formamide because of the N-substitution, and hence, the solution pH is increased more gently, which allows us to control both the gelation and the structural development of phase separation. Another obstacle is related to thermal stability of micro and mesoporous structures. As will be described below, the alkoxy-derived sol–gel process accompanied by phase separation and subsequent aging in the mother liquor produce amorphous ZrO_2 monolithic gels with well-defined macropores and microstructured skeletons. The surface area of about 108 $m^2\ g^{-1}$ was obtained in the amorphous dried gel; however, when the dried gel were heated to crystallize (~400 °C), an abrupt decrease in surface area occurred due to collapse of microporous structures. In other words, high-surface-area, crystalline ZrO_2 with multiscale porous structures could not be obtained through aging in the mother liquor at 80 °C. Some researches on synthesis of ZrO_2 using the metal alkoxides or salts as precursors demonstrated that the solvothermal method in which organic media are adopted instead of water in the hydrothermal method favors the formation of thermally stable, crystalline phases with a high surface area, although the products are obtained in the form of powders.[26–28] For example, Inoue et al.[28] reported that the thermal decomposition of zirconium precursors in organic media such as glycols and toluene at 300 °C can afford nanocrystalline tetragonal ZrO_2 powders (4–10 nm in diameter) and that these materials maintain relatively high surface areas (90–160 $m^2\ g^{-1}$) even after heat treatment at 500 °C. Based on these experimental results, we here attempt to design both the micro and/or mesoporous structures and crystallinity of macroporous ZrO_2 monolithic gels using the solvothermal treatment as a postgelation aging process; namely, the as-gelled wet ZrO_2 specimens with bicontinuous network on the micrometer range are subjected to solvent exchange with an alcohol, followed by heat treatment in a closed vessel (autoclave). Since the bicontinuous macroporous channels enhance the material transport within the monolithic gel, the exchange of pore liquid with an external solvent takes place readily at the stage of wet state. It is anticipated that physicochemical reactions during the solvothermal treatment exert some significant effects on the microstructure and crystal structure. We show that the solvothermal treatment is effective in tailoring the mesotexture and crystallinity without affecting the preformed macroporous morphology. One can obtain high-surface-area, crystalline ZrO_2 monoliths with precisely controllable macropores and thermally stable, mesostructured ZrO_2 skeletons by combining the well-

(15) Tanaka, N.; Kobayashi, H.; Ishizuka, N.; Minakuchi, H.; Nakanishi, K.; Hosoya, K.; Ikegami, T. *J. Chromatogr., A* **2002**, *965*, 35.
(16) Tanaka, N.; Kobayashi, H.; Nakanishi, K.; Minakuchi, H.; Ishizuka, N. *Anal. Chem.* **2001**, *73*, 420A.
(17) Minakuchi, H.; Nakanishi, K.; Soga, N.; Ishizuka, N.; Tanaka, N. *J. Chromatogr., A* **1997**, *762*, 135.
(18) Minakuchi, H.; Nakanishi, K.; Soga, N.; Ishizuka, N.; Tanaka, N. *Anal. Chem.* **1996**, *68*, 3498.
(19) Ishizuka, N.; Kobayashi, H.; Minakuchi, H.; Nakanishi, K.; Hirao, K.; Hosoya, K.; Ikegami, T.; Tanaka, N. *J. Chromatogr., A* **2002**, *960*, 85.
(20) Livage, J.; Henry, M.; Sanchez, C. *Prog. Solid State Chem.* **1988**, *18*, 259.
(21) Yoldas, B. *J. Mater. Sci.* **1986**, *21*, 1087.
(22) Sanchez, C.; Livage, J.; Henry, M.; Babonneau, F. *J. Non-Cryst. Solids.* **1988**, *100*, 65.
(23) Kallala, M.; Sanchez, C.; Cabane, B. *J. Non-Cryst. Solids.* **1992**, *147*, 189.
(24) Konishi, J.; Fujita, K.; Nakanishi, K.; Hirao, K. *Chem. Mater.* **2006**, *18*, 6069.
(25) Backlund, S.; Smått, J. H.; Rosenholm, J B.; Linde′n, M. *J. Dispersion Sci. Technol.* **2007**, *28*, 115.
(26) Wang, X.; Lorimer, G.; Xiao, P. *J. Am. Ceram. Soc.* **2005**, *88*, 809.
(27) Hua, Z.; Wang, X.; Xiao, P.; Shi, J. *J. Eur. Ceram. Soc.* **2006**, *26*, 2257.
(28) Inoue, M.; Kominami, H.; Inui, T. *Appl. Catal., A* **1993**, *97*, L25.

Table 1. Starting Compositions of $Zr(O^nPr)_4-HNO_3-H_2O-NFA-PEO$ System[a]

$Zr(O^nPr)_4$	65 wt % HNO_3(aq)	H_2O	NFA	PEO (M_n = 35 000)
9.36	2.30	6.96	2.88	P^b

[a] All units are grams. [b] P was varied from 0.04 to 0.150.

controlled alkoxy-derived sol–gel process with the solvothermal process.

Experimental Section

Chemicals. Zirconium propoxide ($Zr(O^nPr)_4$, Aldrich) was used as a zirconium source, and a mixture of distilled water (H_2O) and 65 wt % aqueous solution of nitric acid (HNO_3, Hayashi Pure Chemical Ind., Ltd.) as the solvent. *N*-Methylformamide (NFA, Wako Pure Chemicals Ind., Ltd.) was added to initiate gelation, and poly(ethylene oxide) (PEO, Aldrich) having a number-average molecular weight (M_n) of 35 000 were used as a polymer to induce the phase separation. All reagents were used as received.

Synthesis. The monolithic gels were prepared from the starting compositions as listed in Table 1. Only the amount of PEO was varied in order to control the phase-separation tendency. Hereafter, the amount of PEO added to the starting solution will be often denoted by P (unit: gram) to distinguish the samples prepared with different PEO contents. The detail of gel preparation is as follows. The aqueous solution containing HNO_3, PEO and NFA was added to $Zr(O^nPr)_4$ while stirring under ice cooled condition. After stirring for 5 min, the resultant homogeneous solution was poured into a test tube. The test tube was sealed and kept at 80 °C for 1 h for gelation. The wet gel thus obtained was subjected to one of the following procedures: (i) aging in the mother liquor at 80 °C for 24 h or (ii) solvent exchange of the mother liquor with absolute ethanol and subsequent solvothermal treatment at temperatures of 170 to 250 °C for 24 h under an autogenous pressure. The solvent exchange with ethanol was initiated about 20 min after gelation. The ethanol was completely renewed every 12 h for a period of 1 day. The solvent-exchanged gel was put into a poly(tetrafluoroethylene) tube and transferred to a stainless-steel autoclave to be treated at elevated temperatures. After solvothermal treatment, the autoclave was cooled down slowly to room temperature. After either of the treatment (i) or (ii), the resultant gel was evaporation-dried at 40 °C for 3 days. For some dried gels, heat treatment was carried out at temperatures between 300 and 900 °C for 5 h in air in order to explore the thermal stability of micro and/or mesostructures.

Characterization. The morphology of gels was observed by scanning electron microscope (SEM, S-2600N, Hitachi Ltd., with Pt coating) and field-emission scanning electron microscope (FE-SEM, JSM-6700F, JEOL Ltd. without coating). High-resolution transmission electron microscope (HRTEM) images were taken with a JEOL JEM2011 electron microscope operating at 200 kV in order to examine the microstructure of gels. To make the specimen for TEM observation, the monolithic gel was ground into fine powders and then sonicated in absolute ethanol to form a slightly turbid suspension. A small drop of the resultant suspension was placed on a carbon-coated cupper mesh grid and dried at room temperature. The size distribution of macropores was determined by mercury porosimetry (PORESIZER-9320, Micromeritics Co.). Mesoporous structures were characterized by a nitrogen adsorption–desorption isotherm (TriStar, Micromeritics Co.). The size distribution of mesopores was calculated from the adsorption branch of the isotherm using the Barrett–Joyner–Halenda (BJH) method, and the surface area was obtained by the Brunauer-Emmet-Teller (BET) method. X-ray diffraction (XRD) patterns were recorded on a Rigaku diffractmeter (Rint2500, Rigaku) using Cu Kα radiation. The measurements were made on the powder specimen prepared by grinding the monolithic gel. The size of crystallites was calculated from the full width at half-maximum of the (011) and (111) diffraction peaks of tetragonal and monoclinic phases, respectively, using Scherrer's equation.

Results and Discussion

Formation and Control of Interconnected Macropores. In all the compositions as described in Table 1, the starting solutions were initially homogeneous and transparent. As time elapsed, the phase separation and the gelation proceeded spontaneously in a closed and static condition at a constant temperature (80 °C). The gelation can be controlled by the addition of NFA under the acidic condition. The reactivity of $Zr(O^nPr)_4$ is significantly reduced in the acidic condition where the solution pH is much lower than the isoelectric point of ZrO_2, pH = 6–7,[29,30] since alkoxy-derived oligomers grown via the hydrolysis and successive condensation are positively charged and stabilized by the repulsive electrostatic interaction in a fashion similar to that observed for colloidal particles-dispersed systems.[31,32] The electrostatic repulsion in turn decreases when NFA is gradually hydrolyzed in the acidic condition to generate aqueous ammonia in situ. The slow and uniform pH rise weakens the electrostatic repulsion, which induces the polycondensation and finally leads to the gelation. The gelation took place after 30 min to 1 h of leaving at 80 °C, depending weakly on the PEO content. Here, it should be mentioned that the use of formamide (FA), instead of NFA, was not effective in the highly reactive alkoxy-derived ZrO_2 systems, although the addition of FA enabled the control of the gelation in the less reactive alkoxy-derived TiO_2 systems as reported previously.[24] For example, the substitution of FA for NFA listed in Table 1 led to a rapid reaction rate due to steep pH rise at 80 °C after mixing the starting materials, resulting in nonuniform gelation. Even when the reaction temperature was decreased down to 30 °C, the gelation time was still very short (a few minutes), which made it difficult to control the structural development of phase separation parallel to gelation. As a result, the addition of NFA to the present alkoxy-derived ZrO_2 systems under the acidic condition is one of key points of inducing the homogeneous gelation throughout the solution. On the other hand, the addition of PEO to the starting solution has a significant effect on the formation of phase-separating structures. The appearance of as-gelled wet specimens changed systematically with PEO content, P, in the starting solution. When P was small, colorless and transparent or white and translucent gels were obtained. As P was increased, the gels became opaque white. The dried gels prepared via aging in the mother liquor at 80 °C were subjected to SEM observation and mercury porosimetry measurements in order to characterize the macroporous structures.

Figure 1 depicts the SEM images of dried gels prepared with varied P. As P is increased, the gel morphology in the

(29) Randon, J.; Larbot, A.; Guizard, C.; Cot, L.; Lindheimer, M.; Partyka, S. *Colloids Surf.* **1991**, *52*, 241.
(30) Tewari, P.; Lee, W. *J. Colloid Interface Sci.* **1975**, *52*, 77.
(31) Derjaguin, B.; Landau, L. *Acta Physicochim.* **1941**, *14*, 633.
(32) Verwey, E.; Overbeek, J. *Theory of Stability of Lyophobic Colloids*; Elsevier: Amsterdam, 1948.

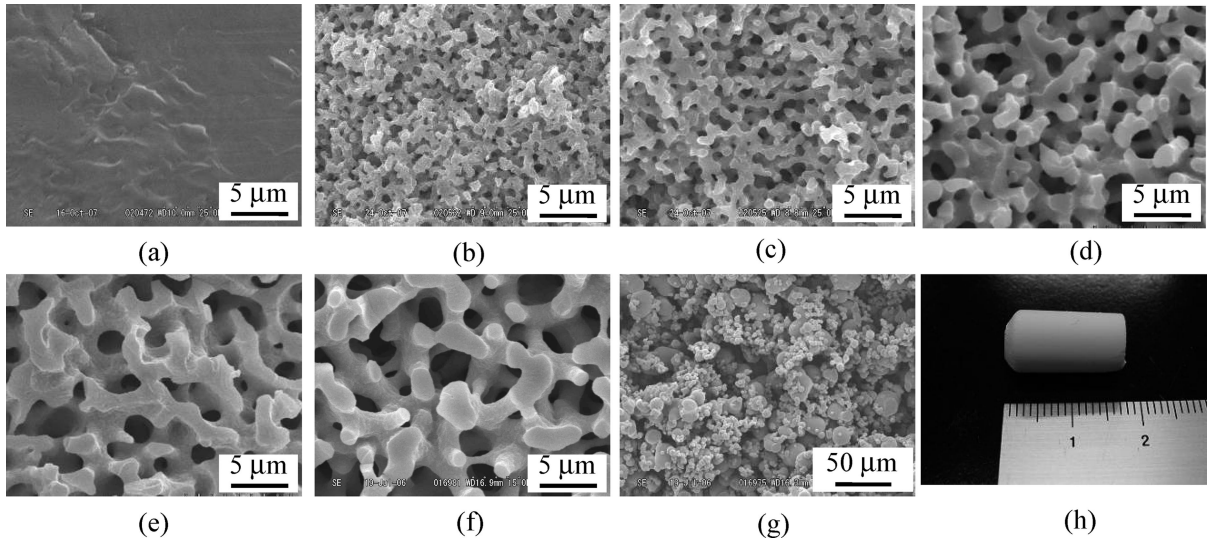

Figure 1. (a−g) SEM images of dried ZrO_2 gels prepared with varied PEO content, $P{:}P$ = (a) 0.040, (b) 0.090, (c) 0.110, (d) 0.115, (e) 0.120, (f) 0.130, and (g) 0.150. (h) Digital picture of monolithic ZrO_2.

micrometer range changes from nonporous [Figure 1 a], through bicontinuous structure with ZrO_2 gel skeletons and interconnected macropores [Figures 1 b−f], to particle aggregates [Figure 1 g]. The variation of gel morphology with P is determined by the onset of phase separation relative to the gelation. The phase separation tendency is related to the miscibility of a polymeric system, which can be estimated by the Flory–Huggins formulation.[33] The Gibbs free energy change of mixing, ΔG, can be described as follows:

$$\Delta G \propto RT\left(\frac{\varphi_1}{P_1}\ln\varphi_1 + \frac{\varphi_2}{P_2}\ln\varphi_2 + \chi\varphi_1\varphi_2\right) \qquad (1)$$

where φ_i and P_i are the volume fraction and the degree of polymerization of component i (i = 1 or 2), respectively, χ is the interaction parameter, R is the gas constant, and T is the temperature. The former two terms in parenthesis represent the entropic contribution, and the last term the enthalpic contribution. It is evident that the polymerization reaction of ZrO_2 oligomers makes ΔG less negative or positive due to the increase in either P_1 or P_2 of eq 1, which destabilizes the system. In the present systems, the positive enthalpic term originated from the repulsive interaction can also contribute to turn ΔG positive. As reported for PEO-incorporated alkoxy-derived SiO_2 sol–gel systems,[13] hydrophobic-hydrophilic repulsive interaction between solvent mixtures and PEO adsorbed on SiO_2 oligomers drives the phase separation due to an increase in the enthalpic term during the polymerization reaction. A similar repulsive interaction is expected to work for the present PEO-incorporated ZrO_2 sol–gel systems, since PEO adsorbs preferentially to ZrO_2 oligomers via hydrogen bonding.[34,35] Thus, the system phase-separates during the polymerization reaction, and the phase-separation tendency is controlled by P. When P is too small, phase separation does not occur effectively until the gelation, and hence, transparent gels with nanometer-sized pores, i.e, nonporous gels in the micrometer range, can be obtained as monoliths [see Figure 1 a]. On the contrary, when P is too large, phase separation enhances significantly, and the minor phase of bicontinuous structures (gel phase in this case) fragments into spherical particles to reduce the interfacial energy [Figure 1g]. Under the limited regions in between these two cases, nearly concurrent phase separation and sol–gel transition take place to produce the bicontinuous monolithic structure [Figure 1b−f], in which each of the gel phase and the fluid phase is three-dimensionally interconnected on the length scale of micrometers. Upon evaporation drying, the fluid phase composed of solvent mixture turns into continuous macropores, and the gel phase becomes ZrO_2 skeletons, although the resultant gels shrink linearly by about 50–60%. As seen from Figure 1h, a monolithic circular cylinder of ZrO_2 gel can be formed in large dimensions (the diameter of top and bottom faces is ∼ 9 mm, and the length is ∼18 mm). Here, it should be noted that the variation of micrometer-sized morphology with P, as shown in Figure 1, is exactly opposite to that observed for the PEO-incorpotrated SiO_2 systems, where the gel morphology in the micrometer range changes from particle aggregates, through bicontinuous structures, to nonporous structures as P is increased,[17] indicating that the phase-separation tendency becomes weak with increasing P. This difference between SiO_2 and ZrO_2 systems may be related to the fact that there exists a critical P where the complex of PEO and alkoxy-derived oxide oligomers is least stable and the phase separation occurs most easily. In the SiO_2 systems, the phase-separation tendency exhibited a maximum at very low P, and the morphological variation was examined in the P-regions well higher than the critical concentration. In such a situation, the phase-separation tendency decreases with increasing P. On the contrary, P used in the present ZrO_2 systems is low and presumably falls on the P-regions lower than the critical concentration. In this case, the phase-separation tendency becomes strong with increasing P.

Figure 2 shows the pore size distributions measured for ZrO_2 dried gels with bicontinuous macropores using a mercury porosimetry. Each of the dried gels possesses a sharp pore size distribution, which is characteristic of structure formation via spinodal decomposition as proven in the

(33) Flory, P. *Principles of Polymer Chemistry*; Cornell University Press: Ithaca, 1971.
(34) Saravanan, L.; Subramanian, S. *J. Colloid Interface Sci.* **2005**, *284*, 363.
(35) Siffert, B.; Li, J. *Colloids Surf.* **1989**, *40*, 207.

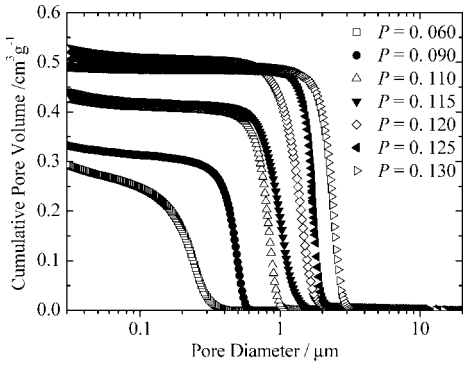

Figure 2. Pore size distributions of the dried ZrO_2 gels prepared with varied PEO content, *P*.

preceding studies.[13] The increase in pore size with an increase in *P* is ascribed to the enhanced phase separation because the spinodal decomposition involves a coarsening process of phase-separating structures.[36,37] As *P* is increased, the compatibility between solvent mixtures and PEO adsorbed on polymerizing ZrO_2 oligomers is reduced, and thus, the onset of phase separation relative to gelation is accelerated to produce the coarsened bicontinuous structure, with large macropores being left behind after evaporation drying. As can be seen from Figure 2, the pore size is controlled between 300 nm to 2 μm by adjusting *P*. Figure 2 also indicates that the pore volume first increases with increasing *P* and then remains unchanged beyond $P = 0.120$. In the course of coarsening process of spinodal decomposition, the bicontinuous structure coarsens self-similarly after the equilibrium compositions of separating phases are reached, so the volume fractions of the gel phase and the solvent mixture-based fluid phase that turns into macropores after evaporation drying should be kept constant irrespective of *P*. In such a situation, the pore volume is independent of *P*. Meanwhile, a significant amount of solvent mixture is still distributed to the gel phase before the phase equilibrium is achieved, which would decrease virtually the relative volume fraction of fluid phase and also increase the degree of gel shrinkage during drying. These duplicate effects are prominent at the low *P*-regions where the phase-separation tendency is weak. As a result, the gels prepared with lower *P* possess the lower pore volume.

The size and volume of bicontinuous macropores can be tailored by other composition parameters as well as *P*. For instance, NFA affects both the sol–gel kinetics and the phase-separation behavior. Starting from the solution with a fixed *P* but higher concentrations of NFA, the polycondensation reaction is accelerated due to more rapid rise in the solution pH. At the same time, it is anticipated that the increase in NFA concentration makes the phase-separation tendency strong, because the repulsive interaction between PEO-adsorbed ZrO_2 oligomers and solvent mixtures is increased due to the high polarity of NFA. The final gel morphology depends on the competitive effects of accelerated polycondensation reaction and enhanced phase separation. We

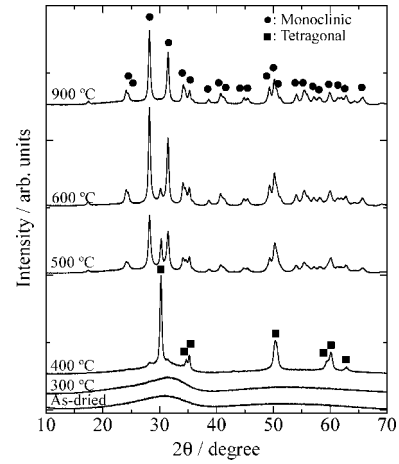

Figure 3. XRD patterns of the dried ZrO_2 gel prepared with $P = 0.110$ and those heat-treated at various temperatures. Symbols ● and ■ represent the diffraction peaks ascribed to the monoclinic and tetragonal phases, respectively.

observed that the gels prepared with higher concentrations of NFA possessed larger-sized bicontinuous macropores, indicating that the enhanced phase separation was more dominant. The amount of NFA also controls the pore volume since the relative volume fractions of gel phase and solvent phase are altered by adding or reducing NFA. A wide variety of structures with desired size and volume of macropores can be designed by adjusting the composition parameters.

Control of Mesostructure and Crystallinity. We first examine the effects of heat treatment on the crystallinity and micro and mesoporous structures of the dried gels shown in Figure 1, i.e., specimens prepared via aging in the mother liquor at 80 °C after gelation. Characterizations using XRD analysis, nitrogen adsorption–desorption isotherms, and SEM and FE-SEM observations were carried out for the dried gel prepared with $P = 0.110$ and those heat-treated at various temperatures.

Variation of XRD pattern with heat-treatment temperature is depicted in Figure 3. Only halo patterns are observed for the dried gel and that heat-treated at 300 °C, indicating that these materials are amorphous to X-ray. Upon heating at 400 °C, broad diffraction peaks appear due to the precipitation of nanocrystals. The crystalline phases consist predominantly of tetragonal ZrO_2 with a small amount of monoclinic ZrO_2. When the heat-treatment temperature is further increased, the fraction of the monoclinic phase increases gradually as a result of the conversion of tetragonal to monoclinic phases. A single phase of monoclinic ZrO_2 is present after heat treatment at 900 °C. The sequence of phase transformation upon heating is quite different from that observed for the bulk counterpart which exists as a monoclinic form at room temperature, undergoes monoclinic to tetragonal transformation at 1175 °C, and exhibits tetragonal to cubic transformation at 2370 °C.[38] Garvie[39]calculated that ZrO_2 is stabilized in the tetragonal form even at room temperature when the crystallite size is less than a critical size, owing to the lower surface energy of tetragonal form compared to monoclinic one. He argued that the critical size of tetragonal stabilization

(36) Hashimoto, T.; Itakura, M.; Shimizu, N. *J. Chem. Phys.* **1986**, *85*, 6773.
(37) Hashimoto, T.; Itakura, M.; Hasegawa, H. *J. Chem. Phys.* **1986**, *85*, 6118.
(38) Mitsuhashi, T.; Fujiki, Y. *J. Am. Ceram. Soc.* **1973**, *56*, 493.
(39) Garvie, R. *J. Phys. Chem.* **1978**, *82*, 218.

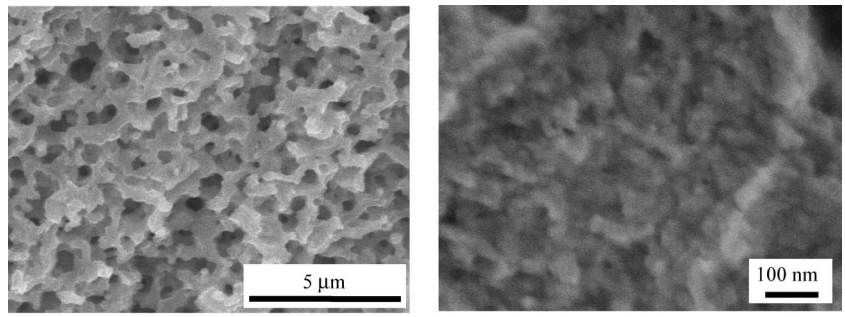

Figure 4. (a) SEM and (b) FE-SEM images of the ZrO_2 gel prepared with $P = 0.110$ and then heat-treated at 400 °C.

for nanoparticle aggregates is 30 nm. For the gels heat-treated at 400 and 500 °C, the crystallite sizes of tetragonal ZrO_2 estimated by Scherrer's equation are 22 and 29 nm, respectively. The tetragonal ZrO_2 is stabilized because the crystallite size is smaller than the critical size calculated under an assumption of nanoparicle aggregates. On the other hand, the crystallite size of the monoclinic ZrO_2 precipitated in the gel heat-treated at 500 °C is estimated to be 20 nm by using Scherrer's equation, which is smaller than that of the coexisting tetragonal ZrO_2. The result is not consistent apparently with the critical size theory in which tetragonal-to-monoclinic phase transformation occurs over the critical size, but may be explained by considering the formation of interfaces inside the monoclinic crystallites grown over the critical size. The intracrystallites interface is caused by twinning and/or lattice strain in monoclinic ZrO_2 nanocrystals, which leads to the underestimation of crystallite size by XRD analysis.[40,41]

The progressive crystallite growth during heat treatment at higher temperatures (>500 °C) facilitates to convert into the thermodynamically stable, monoclinic ZrO_2. Figure 4 a,b displays the SEM and FE-SEM images of the gel heat-treated at 400 °C, respectively. Well-defined bicontinuous macroporos morphology is maintained after heat treatment, while ZrO_2 nanoparticles comprising of gel skeletons are nonuniformly distributed, implying the particle growth via hard aggregation during heat treatment.

Nitrogen adsorption–desorption isotherms and the corresponding BJH pore size distributions are shown in Figure 5 a,b, respectively, for the dried gel and those heat-treated at 300 and 400 °C. The isotherm of dried gel is of type I according to the IUPAC classification, signifying the existence of micropores. The median pore size is estimated to be about 1.8 nm as revealed from the BJH pore size distribution, although pores are broadly distributed over the micro to mesoporous regimes. The BET surface area is 108 $m^2\ g^{-1}$. Following heat treatment at temperatures as low as 300 °C, pores on the micro to meso-scales disappear almost completely, and the surface area decreases to about 10 $m^2\ g^{-1}$ [see the inset of Figure 5b]. Obviously, the high-surface-area, crystalline ZrO_2 with multiscale porous structures can not be obtained through the aging process in the mother liquor at 80 °C after gelation, as revealed from the comparison of Figures 3 and 5. The collapse of micro and mesopores and concomitant loss of surface area can be related to the particle growth via hard crystallite aggregation during heat treatment as displayed in Figure 4 b. A similar phenomenon was observed for ZrO_2 powders prepared by precipitation of aqueous zirconium salts or alkoxide solutions, followed by heat treatment at elevated temperature in air.[42] Another postgelation process is thus required to inhibit the hard aggregation of ZrO_2 nanoparticles during drying and heat treatment.

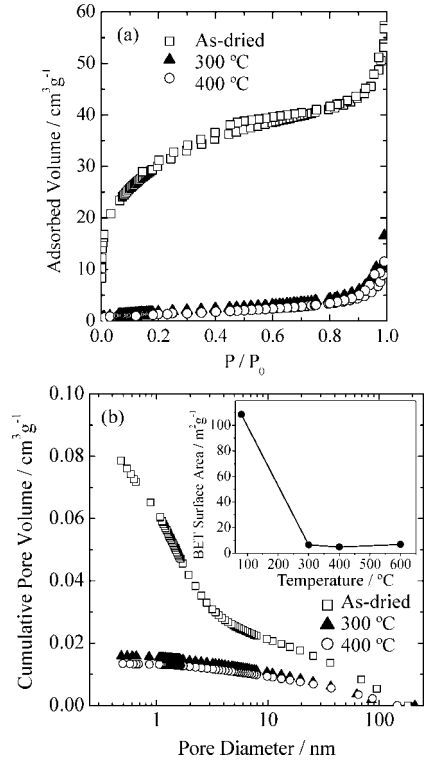

Figure 5. Mesoscale characterizations of the ZrO_2 gels prepared with $P = 0.110$: (a) Nitrogen adsorption–desorption isotherms of the dried gel (□) and those heat-treated at 300 °C (▲) and 400 °C (○). (b) Pore size distributions of the dried gel and those heat-treated at 300 and 400 °C. Symbols are the same as in (a). The inset shows the variation of BET surface area with heat-treatment temperature.

Next, we investigate the effects of postgelation treatment on bicontinuous macroporous ZrO_2 wet gels using a solvothermal process in order to obtain the crystalline ZrO_2 without spoiling the micro and/or mesostructures that afford

(40) Srinivasan, R.; Rice, L.; Davis, B. *J. Am. Ceram. Soc.* **1990**, *73*, 3528–3530.
(41) Guo, G.; Chen, Y. *Appl. Phys. A: Mater. Sci. Process.* **2006**, *84*, 431.
(42) Lerot, L.; Legrand, F.; Debruycker, P. *J. Mater. Sci.* **1991**, *26*, 2353.

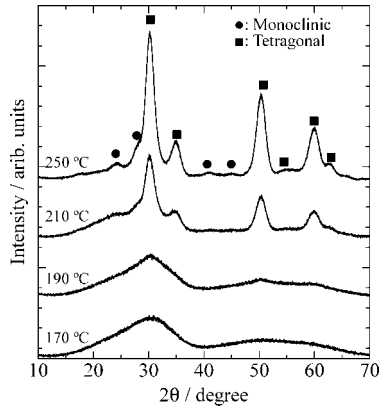

Figure 6. XRD patterns of the dried ZrO_2 gels prepared from the system with $P = 0.110$ via solvothermal treatment at 170, 190, 210, and 250 °C. Symbols ● and ■ represent the diffraction peaks ascribed to the monoclinic and tetragonal phases, respectively.

a large surface area. The solvothermal method has been extensively utilized as a low-temperature processing to produce nanoscale materials in an organic medium under a high pressure like 1 MPa or so, and offers many advantages including the control of morphologies, sizes and phase transformation.[43] The choice of appropriate organic solvents plays a key role in the solvothermal synthesis, because the solvent properties such as redox, polarity, complexation and viscosity, and so forth, strongly influence the heterogeneous liquid–solid reactions. So far, it has been reported that high-surface-area ZrO_2-based powders composed of small, uniform, highly crystallized nanoparticles can be prepared by thermal decomposition of the corresponding metal alkoxides or salts in the presence of organic solvents.[26,27,44] The use of solvothermal treatment as the postsynthesis process has also proven useful in tailoring the porous texture and crystallinity of ZrO_2-based nanoparticles.[45,46] In this study, the aging of wet gels utilizing the solvothermal method was performed by using ethanol as the organic medium. Ethanol was chosen as the organic medium for solvothermal treatment, because either washing of hydrous gels with ethanol or synthesis of gels in ethanolic solution exerted great impact on the inhibition of hard aggregation among ZrO_2 particles during drying and heat treatment.[47,48] Thus, the wet gels prepared with $P = 0.110$, which possessed a bicontinuous structure on the length scale of the micrometers, were fully solvent-exchanged with ethanol and then solvothermally treated at temperatures between 170 and 250 °C before evaporation drying at 40 °C. The resultant dried gels were characterized by HRTEM as well as XRD analysis, nitrogen adsorption–desorption isotherms and FE-SEM observation.

Figure 6 shows the XRD patterns for the dried gels prepared via the solvothermal process at various temperatures. A halo pattern showing X-ray amorphous structure is detected for the dried gel prepared via the solvothermal treatment at 170 °C. Crystallization starts at 190 °C, and the precipitation of tetragonal ZrO_2 is clearly observed at 210 °C. The solvothermal treatment at 250 °C enhances the crystallinity, although a small amount of monoclinic ZrO_2 is precipitated. The comparison between Figures 3 and 6 reveals that the onset temperature of crystallization is lower for the solvothermally treated specimens than for the heat-treated specimens prepared through aging in the mother liquor at 80 °C. Also, the diffraction peaks of tetragonal ZrO_2 observed for the solvothermally treated specimens are much broader than those for the heat-treated specimens prepared through aging in the mother liquor at 80 °C, indicating the smallness of crystallites precipitated. The crystallite sizes of the tetragonal ZrO_2 precipitated in the specimens solvothermally treated at 210 and 250 °C are evaluated to be 7 and 10 nm, by using Scherrer's equation, respectively. HRTEM images (see Figure 7) also demonstrate that the crystallinity is higher with increasing the treatment temperature, with the particle size being dependent weakly on the treatment temperature. For both the specimens solvothermally treated at 210 and 250 °C, the particle size is approximately 8 nm, which is in good agreement with the crystallite size estimated by XRD analysis.

Nitrogen adsorption–desorption isotherms and the BJH pore size distributions are shown in Figure 8 a,b, respectively, for dried gels prepared via the solvothermal process at 170, 210 and 250 °C. Each of the isotherms exhibits a type-IV isotherm, signifying the existence of mesopores. Compared to the case of the specimens prepared through aging in the mother liquor at 80 °C (see Figure 5), pores are more sharply distributed in the mesoporous regime. Dependences of the BET surface area and average mesopore diameter on the temperature of solvothermal treatment are shown in the inset of Figure 8 b. With increasing the treatment temperature from 170 to 250 °C, the surface area increases, exhibits a maximum at 190 °C, and then decreases. Following the solvothermal treatment at temperatures above 210 °C where nanocrystalline tetragonal ZrO_2 is precipitated, the surface area exceeds 200 $m^2\ g^{-1}$. On the other hand, the average diameter of mesopores increases monotonically from 2.5 to 4.8 nm as the treatment temperature is raised from 170 to 250 °C. Thus, the application of solvothermal treatment to as-gelled wet state is effective in tailoring the porous textures as well as crystallinity. Figure 9 a−c display the FE-SEM images of dried gels prepared via the solvothermal process at 170, 210, and 250 °C. The skeletons of macroporous network are comprised of aggregates of finely and uniformly distributed particles. No remarkable change in particle size is observed among specimens prepared via the different solvothermal conditions, which is consistent with the result of TEM observation (see Figure 7). In comparison with the average pore size estimated from the BJH pore size distributions demonstrated in Figure 8, the voids of the aggregated particles work as accessible mesopores. Here, it is worthy to stress that the macroporous morphology is less susceptible to the solvothermal treatment. An example is given in Figure 9 d showing the micrometer-range morphology of the dried gel derived via the solvothermal process at 250 °C. One can see that the solvothermally treated ZrO_2 gel possesses well-defined macropores. The formation of mesopores during the

(43) Dubois, T.; Demazeau, G. *Mater. Lett.* **1994**, *19*, 38.
(44) Štefanić, G.; Musić, S.; Molćanov, K. *J. Alloys Compd.* **2005**, *387*, 300.
(45) Schmidt, T.; Mennig, M.; Schmidt, H. *J. Am. Ceram. Soc.* **2007**, *90*, 1401.
(46) Metelkina, O.; Husing, N.; Pongratz, P.; Schubert, U. *J. Non-Cryst. Solids* **2001**, *285*, 64.
(47) Stöcker, C.; Schneider, M.; Baiker, A. *J. Porous Mater.* **1995**, *2*, 171.
(48) Mercera, P.; Vanommen, J.; Doesburg, E.; Burggraaf, A.; Ross, J. *J. Mater. Sci.* **1992**, *27*, 4890.

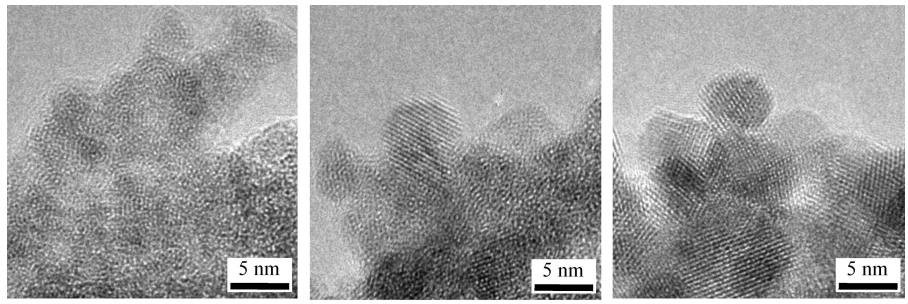

Figure 7. TEM images of the dried ZrO_2 gels prepared from the system with $P = 0.110$ via solvothermal treatment at (a) 170, (b) 210, and (c) 250 °C.

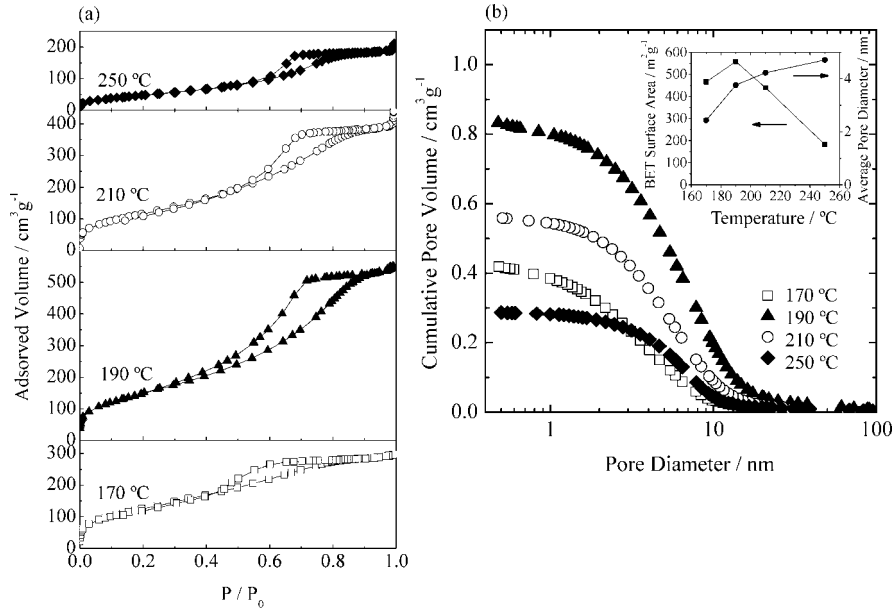

Figure 8. Mesoscale characterizations of the ZrO_2 gels prepared with $P = 0.110$. (a) Nitrogen adsorption–desorption isotherms of the dried gels prepared via solvothermal treatment at 170 °C (□), 190 °C (▲), 210 °C (○), and 250 °C (♦). (b) Pore size distributions of the dried ZrO_2 gels prepared via solvothermal treatment at 170, 190, 210, and 250 °C. Symbols are the same as (a). The inset shows the variations of BET surface area (■) and average pore diameter (●) with temperature of solvothermal treatment.

solvothermal treatment takes place within the preformed micrometer-sized gel skeletons, so the size of mesopores can be controlled independently of the size of macropores.

A remarkable effect of the solvothermal treatment is that the growth of ZrO_2 nanoparticles via hard aggregation is suppressed as demonstrated in Figure 9. In the as-gelled wet state, many nonreacted groups exist on the surface of primary particles comprising the gel skeletons of bicontinuous macroporous network. Most of nonreacted groups are considered to be hydroxy groups, because the hydrolysis reaction is enhanced by the high concentration ratio of H_2O to $Zr(O^nPr)_4$ in the strongly acidic condition. It has been proved that part of hydroxy groups is replaced by ethoxy groups after solvent exchange with ethanol.[49] During the solvothermal treatment, the remaining Zr-OH groups form well-built neck via chemical bonds between adjacent particles, while the particle growth via hard aggregation is inhibited by the surface passivation due to the presence of $Zr\text{-}OC_2H_5$ groups. Owing to the soft aggregation of primary particles, accessible mesopores are formed, and the structural rearrangement accompanied by crystallization can take place mainly inside particles. In addition, the sintering effect during the solvothermal treatment suppresses the collapse of micro and mesopores by subsequent drying, yielding a high surface area. The decrease in surface area for specimens prepared via the solvothermal conditions above 210 °C may be caused by the decrease in micro and mesopores, which originates from the slight growth of crystallites accompanied by phase transformation and also from the intercrystallite sintering that leads to neck growth. Studies on the solvothermal treatment in the presence of a different kind of organic solvent are now in progress in order to clarify definitely the role of solvothermal effect.

Finally, we examine the thermal stability of mesoporous structures for the solvothermally treated gels. When the specimens prepared via the solvothermal process at 210 °C were heat-treated at 400 and 500 °C in ambient atmosphere, the predominant crystalline phase is tetragonal ZrO_2. The surface area was as high as 100 $m^2\ g^{-1}$ after heat treatment at 400 °C, and the specimen heat-treated at 500 °C still retained a surface area of 75 $m^2\ g^{-1}$.

ZrO_2 and TiO_2 are far more stable toward extremes in acidity and alkalinity than SiO_2[50] and have an ability of selectively adsorbing phosphorylated molecules such as

(49) Kaliszewski, M.; Heuer, A. *J. Am. Ceram. Soc.* **1990**, *73*, 1504.
(50) Nawrocki, J.; Dunlap, C.; Carr, P.; Blackwell, J. *Biotechnol. Prog.* **1994**, *10*, 561.

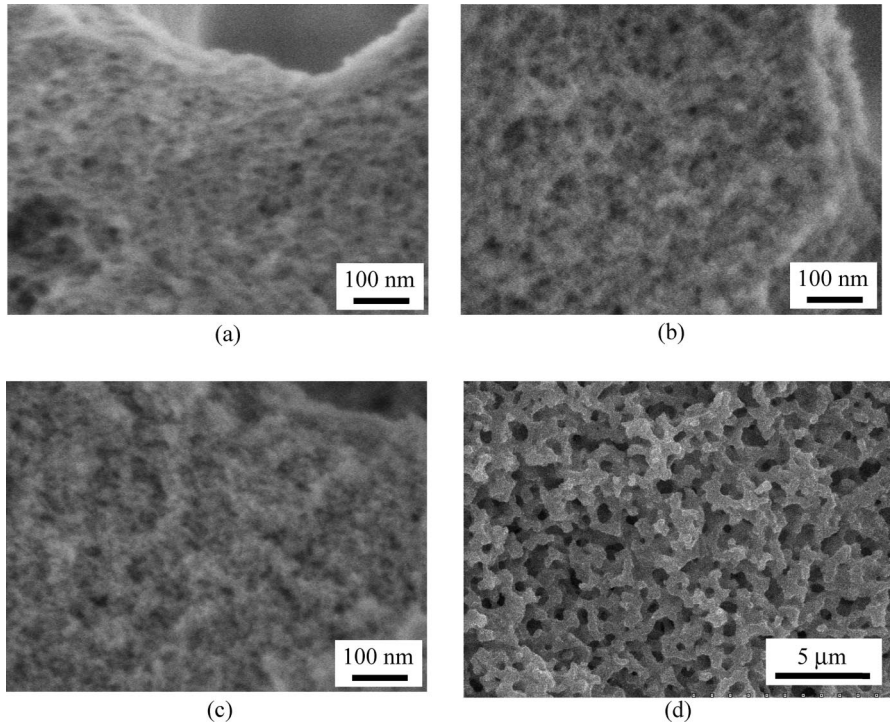

Figure 9. (a−c) FE-SEM images of the dried ZrO_2 gels prepared from the system with $P = 0.110$ via the solvothermal treatment at (a) 170, (b) 190, and (c) 250 °C. (d) SEM image of (c).

peptides and proteins.[51–53] For some phosphorylated molecules, the affinity is different between TiO_2 and ZrO_2; ZrO_2 can adsorb the specific compounds that have low affinity to TiO_2, and vise versa.[54] Thus, the techniques of fabricating macro-mesoporous monoliths for ZrO_2 as well as TiO_2 will be useful for molecular separation in the field of biochemistry. In addition, the tetragonal phase of ZrO_2 has both acidic and basic properties[55] and gives the most active catalyst for some catalytic reactions.[56] As a result, macro-mesoporous tetragonal ZrO_2 monoliths are also expected to find some applications in the fields of catalyst and catalyst–support.

Conclusions

ZrO_2 monolithic gels with well-defined macropores have been prepared via the sol–gel process accompanied by phase separation, and the effects of different postgelation treatment methods, i.e., aging in the mother liquor at 80 °C or solvothermal treatment in ethanol, on the micro and mesoporous structures and crystallinity have been investigated. Polymerization-induced phase separation and concurrent gelation produce the monolithic ZrO_2 gels with well-defined bicontinuous macropores, and the size of macropores can be controlled from 300 nm to 2 μm by adjusting the starting composition. The dried gels obtained through aging in the mother liquor at 80 °C possess the microporous amorphous network and yield a surface area of about 100 $m^2\ g^{-1}$, whereas heating at elevated temperatures (>400 °C), which leads to the precipitation of ZrO_2 crystal, causes the collapse of micropores and concomitant loss of surface area. On the other hand, solvent exchange of the mother liquor in as-gelled wet specimens with ethanol and subsequent solvothermal treatment at temperatures above 210 °C result in the formation of mesoporous structures and the conversion into the crystalline phases, without disturbing the macroporous morphology. Since the formation of mesopores during the solvothermal treatment takes place within the preformed micrometer-sized gel skeletons, the size of mesopores can be controlled independently of the size of macropores. The surface area of the macro-mesoporous crystalline ZrO_2 gels prepared via the solvothermal treatment exceeds 200 $m^2\ g^{-1}$. The production of high-surface-area, crystalline ZrO_2 can be related to inhibition of particle growth via hard aggregation during the solvothermal treatment. The thermal stability of pores in the micro to mesoporous regimes is also improved by the solvothermal treatment; for the dried gels prepared via the solvothermal treatment at 210 °C, the surface areas of 100 and 75 $m^2\ g^{-1}$ can be obtained after heat treatment at 400 and 500 °C, respectively.

Acknowledgment. This study was financially supported by the Grand-in-Aid for Scientific Research (No. 18360316) from the Ministry of Education, Culture, Sport, Science, and Technology (MEXT), Japan, and the Industrial Technology Research Grant Program (04A25023c) and a Grant for Practical Application of University R&D Results under the Matching Fund Method from the New Energy and Industrial Technology Development Organization (NEDO), Japan. K.F. appreciates the research grant from The Mazda Foundation, and J. K. thanks the Grant-in-Aid for Fellow (No. 17・2224) from Japan Society of the Promotion Science (JSPS).

CM703351D

(51) Wirth, H.; Hearn, M. *J. Chromatogr.* **1993**, *646*, 143.
(52) Pinkse, M.; Uitto, P.; Hilhorst, M.; Ooms, B.; Heck, A. *Anal. Chem.* **2004**, *76*, 3935.
(53) Matsuda, H.; Nakamura, H.; Nakajima, T. *Anal. Sci.* **1990**, *6*, 911.
(54) Sugiyama, N.; Masuda, T.; Shinoda, K.; Nakamura, A.; Tomita, M.; Ishihama, Y. *Mol. Cell. Proteomics* **2007**, *6*, 1103.
(55) Yamaguchi, T. *Catal. Today* **1994**, *20*, 199.
(56) Centi, G.; Cerrato, G.; DAngelo, S.; Finardi, U.; Giamello, E.; Morterra, C.; Perathoner, S. *Catal. Today* **1996**, *27*, 265.